



An Investigation of the Effect of Adding KSCN on the UV-Visible Absorption Behaviour of Chitosan-based Iodophor

NAOREM SHUBHASCHANDRA SINGH^{1*}, CH SHANTI DEVI²,
S MANIMUKTA DEVI² and W HARIMATI DEVI³

¹Department of chemistry Dhanamanjuri University Manipur-795001, India.

²Department of Chemistry, Naorem Birahari College Khundrakpam, Manipur-795114, India.

³Department of Chemistry, Manipur University Canchipur, Manipur-795003, India.

*Corresponding author E-mail: Shubhasnaorem@dmu.ac.in

<http://dx.doi.org/10.13005/ojc/400411>

(Received: March 22, 2024; Accepted: July 24, 2024)

ABSTRACT

Electronic spectral analysis of a tri-iodide solution in an acetic acid medium revealed the presence of strong absorption bands for tri-iodide at 287.5 and 351.5nm. A notable shift in the absorption band to 310nm indicated the formation of a complex between Chitosan and tri-iodide in an acidic medium solution. Chitosan-tri-iodide complex formation was significant at concentrations >0.5% (w/v). At lower concentrations, weak complexation is evident through the comparatively lower absorption of the iodophors. The introduction of KSCN to the polymer-iodophor system leads to a gradual reduction in absorption over time and is completed within 1 hour. If polymer mixtures of (1:1) ratio were used in iodophor, it persists as complex iodophor for a longer period. Photoluminescence investigations show sharp and narrow emission peaks at 350.5 and 701.5nm, highlighting unique fluorescent species alongside effective radiative recombination. It minimizes energy dissipation and suggests promising fluorescence applications across diverse fields.

Keywords: Chitosan, Polyvinyl pyrrolidone (PVP), Polyvinyl alcohol (PVA), Iodophore, UV-visible spectra, Photoluminescence spectra etc.

INTRODUCTION

Chitosan (Cs) is a polymer with a random distribution of β -(1-4)-linked D-glucosamine and N-acetyl-D-glucosamine within the polymer soluble in both organic and dilute mineral acids.^{1,2} Chitosan and its derivatives have diverse bioactivities, non-toxicity, low allergenicity, biocompatibility, antitumor, antimicrobial, and antioxidant activities in water treatment, wound healing materials,

pharmaceutical excipients or drug carriers, obesity treatment, and as a scaffold for tissue engineering biodegradability^{3,4} etc. Chitosan is sometimes modified to increase antibacterial activity and solubility while decreasing intermolecular H-bonding.⁵ Chitosan-based iodophors form while chitosan complexes with iodine. They are also kinetically unstable and decompose at room temperature. Chitosan iodophors show intense absorption bands of tri-iodide and iodate ions,



polyiodide ions, bound to the macromolecule using hydroxyl group at C1, C3 and C4.^{6,7} The formation of Chitosan iodophors increases by incorporating the system with hydroiodic salts and polyols.⁸ Thiocyanate (SCN⁻) induces decolourization of the Chitosan–iodophore by interrupting the available ions within the system. This interference extends to the formation of the starch-iodine complex.⁹ Potassium thiocyanate is a compound widely used in various pharmaceutical formulations and antifungal treatments and also enhances the antifungal activity of chitosan-iodophors.^{10,11} However, no literature exists regarding the optimization of chitosan (or chitosan+polymer mixture)-iodophore formulation, the stability and kinetics or the degradation pathways of the iodophore systems necessary for effective bio-compatibility applications while interacting with biological systems. Therefore, we consider the aforementioned areas as potential avenues for further study.

The present study aims to examine the absorption behaviour of Chitosan-based iodophors in a 2% w/v acetic acid solution at varying concentrations of iodine or chitosan. Additionally, we will assess the changes in the absorption maximum of the complexes on the addition of KSCN, narrowing down the gap of potential research avenues.

MATERIALS AND METHODS

Chitosan (Cs), iodine (I₂), KI, and KSCN were used in this study. Cs, KI and iodine (I₂) molecules were obtained from pure Hi-Media. KSCN was procured from SD Fine Chemical Ltd. The polymers and other samples used in this study were of A (analytical) grade products and used as received without further treatment. The structures of Chitosan (Cs), polyvinyl pyrrolidone (PVP), and hydroxyl propylcellulose (HPC) are shown in Figure 1.

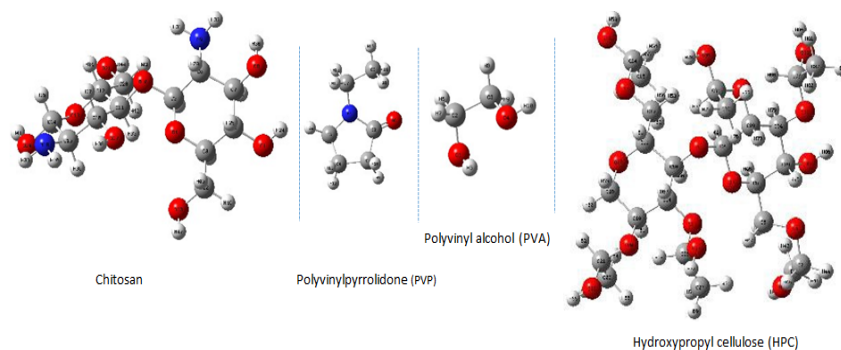


Fig. 1. 3D structures of different polymers used in the present study

Preparation of the solution

All solutions were carefully prepared by dissolving a precisely measured quantity of the solute in a known amount of solvent. Stock solutions of approximately 5% (w/v) Cs, 2% (w/v) HPC, and 2% (w/v) PVP were prepared by dissolving the polymers in a 100 mL volumetric flask containing 2% (w/v) acetic acid solution. The dissolution process was performed by allowing the solutions to stand for about 48 h at room temperature to obtain a clear solution. Subsequently, solutions for lower concentrations were prepared through the dilution method. Similarly, 20mM I₂/KI (1:4) and 2% (w/v) KSCN were also prepared in a 100 mL volumetric flask by dissolving them in a 2% acetic acid solution, following the methods consistent with the preparation of other solutions.

Preparation of Chitosan-iodophor

An adequate amount of 5% (w/v) Cs from the stock solution was mixed with I₂/KI solution to obtain various predetermined concentrations of Cs and I₂/KI solution in a 2% (w/v) acetic acid. Subsequently, the mixture was allowed to stand at room temperature for approximately 10 min to facilitate further UV-Visible spectrophotometric measurements. KSCN was introduced to a 10 mL volumetric flask containing a predetermined concentration of Cs and I₂/KI solutions, resulting in a final concentration of 0.02% w/v KSCN in a 2% (v/v) acetic acid solution to investigate its impact.

UV-Visible Measurement

The UV-Visible absorption spectra of the Cs–based iodophors at a fixed concentration of

I_2/KI solution for different concentrations of Cs were recorded using a Shimadzu UV-1900i UV-Visible spectrophotometer in the range 250-600nm in both the absence and presence of KSCN. Various spectra of the same iodophor were also recorded at different concentrations of I_2/KI /iodide solution while maintaining a fixed Cs concentration. Absorption spectra of the Cs-based iodophor were recorded after blending with polymers such as PVP and HPC following the addition of KSCN within the wavelength range of 250-700nm at room temperature.

Photoluminescence (PL) Measurement

The photoluminescence emission spectra of the I_2/KI /iodide solution and Cs-based iodophor for different Cs concentrations at 0.1mM I_2/KI /iodide acidic solution were recorded using a Hitachi F-4700 Fluorescence Spectrophotometer in the range 280-800nm at a scan speed of 240nm/min at room temperature. The emission spectra were excited at 700nm.

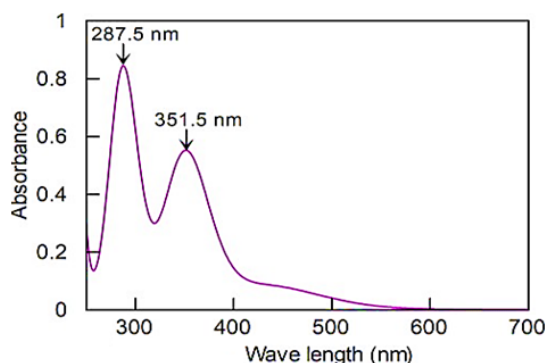


Fig. 2. UV-Visible Spectra of I_2/KI solution in 2%(v/v) acetic acid

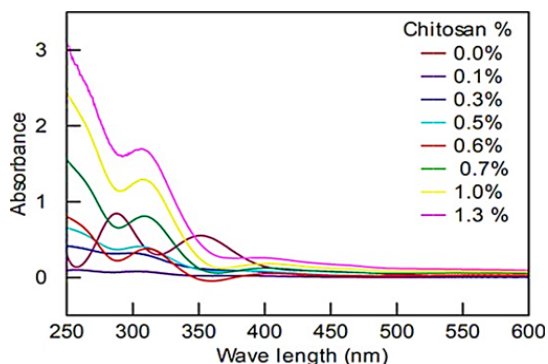


Fig. 4. UV-Visible Spectra Chitosan-iodophore complex at different chitosan concentration

RESULTS

Figure 2 illustrates the UV-Visible spectra of 0.1mM iodine (I_2/KI) solutions in 2% (w/v) acetic acid. The absorption maxima were observed between 287.5 and 351.5nm. Fig. 3 shows the UV-Visible absorption spectra of the Cs iodophor solutions at different Cs concentrations, while maintaining an iodine concentration of 0.1mM. The iodophor exhibited two absorption peaks at ~287.5 and 351.5nm without much change from the absorption peaks observed in I_2/KI solution. The complexation between Cs and iodine is evident from the appearance of new absorption maxima at 310nm and the disappearance of both the absorption maxima at 287 and 351nm Fig. 4. The behaviour of the absorbance of the iodophor complex for different Cs concentrations at 310nm is presented in Fig. 5. Complexation between Cs and iodine increases with Cs concentration as the absorption maxima increases with Cs content and shows some anomaly at around 0.5% w/v of Cs Figures 4 & 5.

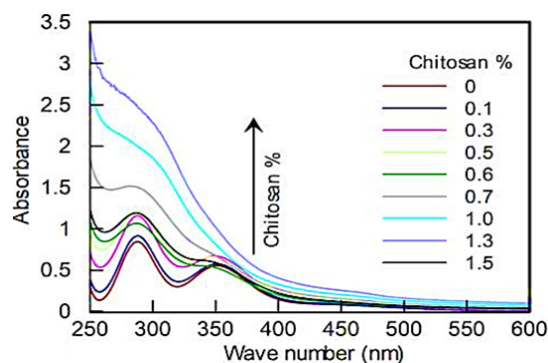


Fig. 3. UV-Visible Spectra of Chitosan-iodophore solution at different Chitosan conc. in 2% (v/v) acetic acid

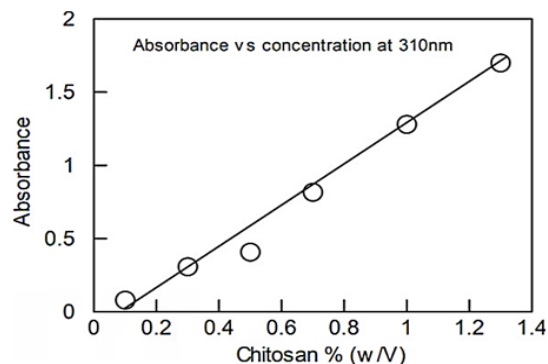


Fig. 5. Variation of Absorbance and Cs concentration for Chitosan-iodophore complex measured at 310nm

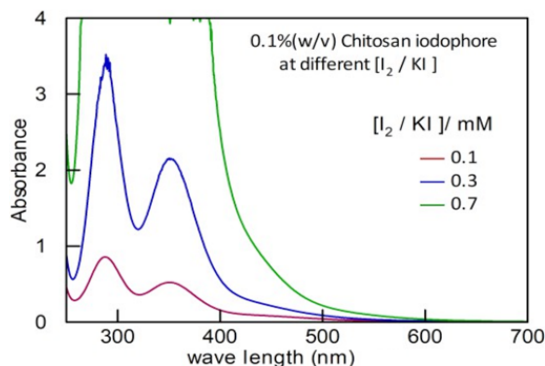


Fig. 6. UV-Visible Spectra of 0.1% (w/v) Cs-iodophore solution for different I_2/KI concentration

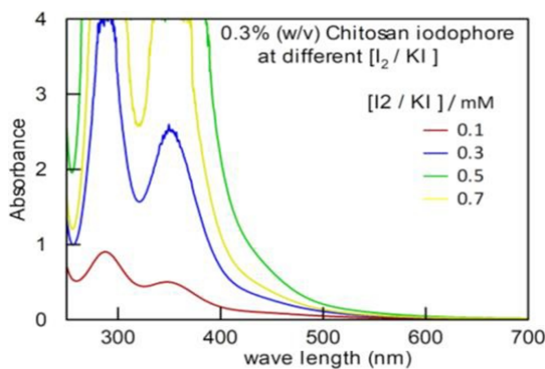


Fig. 7. UV-Visible Spectra of 0.3% (w/v) Cs-iodophore solution for different $[I_2/KI]$

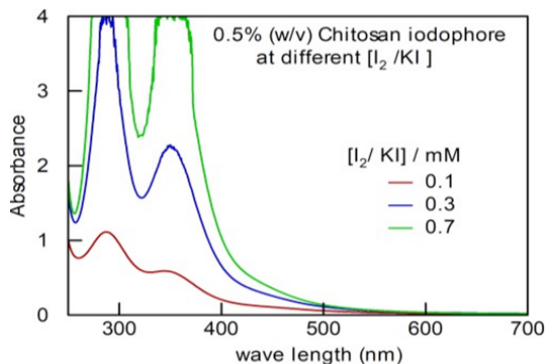


Fig. 8. UV-Visible Spectra of 0.5% (w/v) Cs-iodophore solution for different $[I_2/KI]$

The UV-Visible absorption spectra of polymer mixture-iodophore solutions are shown in Fig. 9-11. The polymer mixtures were prepared between Cs and HPC, Cs and PVP, and Cs and PVA by maintaining the composition of the polymer in a 1:1 ratio. The Cs+PVP (1:1)-iodophore solution of 0.1% (w/v) polymer mixture has shown prominent absorption maxima at ~292 and 368nm, Fig. 9. The two absorption maxima start diminishing from 0.3% (w/v) polymer mixture and beyond, observe

no absorption maxima or peaks. Such UV-Visible spectra are also observed in the iodophores of other polymer mixtures of Cs+HPC and Cs+PVA Figures 10 & 11.

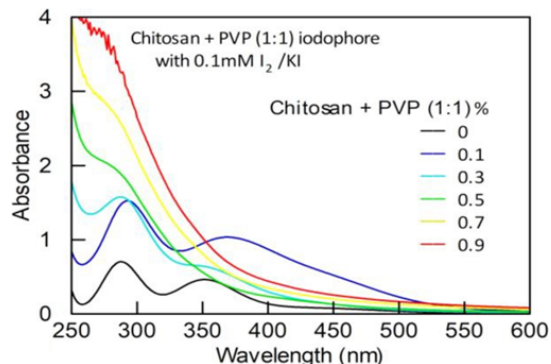


Fig. 9. UV-Visible Spectra of Cs+PVP (1:1)-iodophore with 0.1mM I_2/KI at different polymer mixture concentration

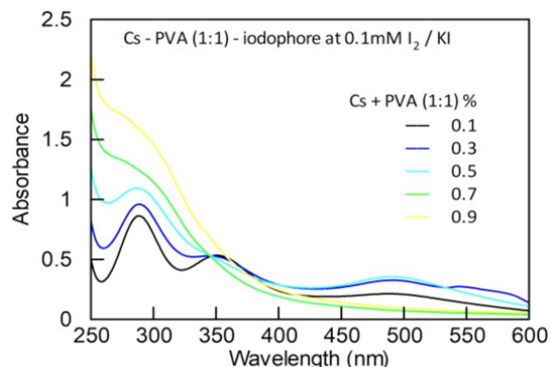


Fig. 10. UV-Visible Spectra of Cs+PVA (1:1)-iodophore at different polymer mixture concentration

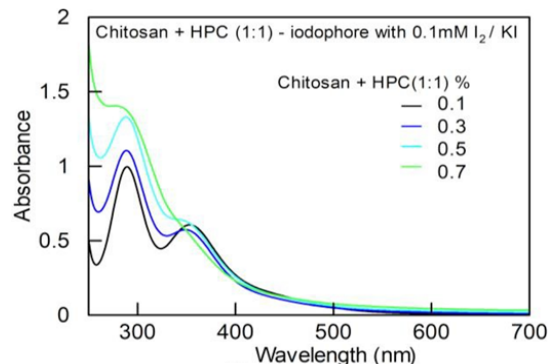


Fig. 11. UV-Visible Spectra of Cs+PVP (1:1)-iodophore at different polymer mixture concentration

UV-Visible spectra of the Cs+PVP (1:1)-iodophore complexes at different concentrations of the polymer mixture are shown in Fig. 12. Higher absorbance values, accompanied by irregular spectral patterns, are evident across various concentrations of the polymer mixture and

I_2/KI solution Fig. 13 and 14. Aberrant formation of polyiodide ions is apparent up to 0.3% w/v of the polymer mixture and 0.3mM of I_2/KI solution.

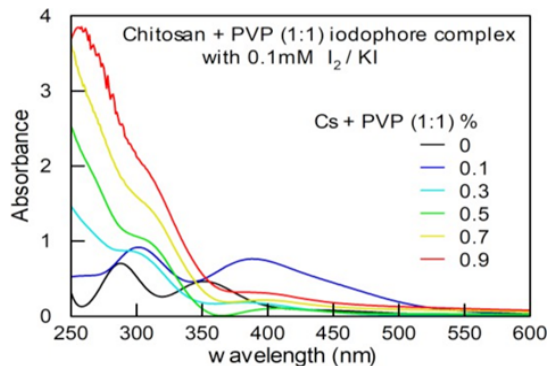


Fig. 12. UV-Visible Spectra of Cs+PVP (1:1)-iodophore complex with 0.1mM I_2/KI at different polymer mixture concentration

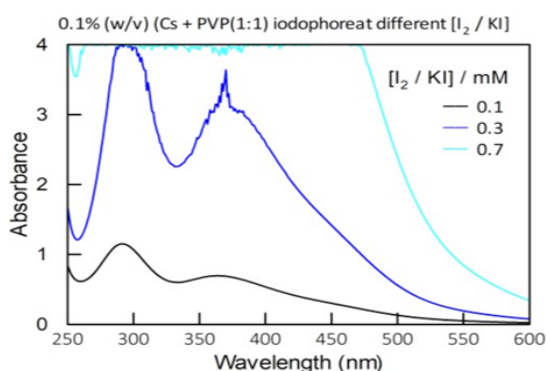


Fig. 13. UV-Visible Spectra of (0.1% w/v) Cs+PVP (1:1)-iodophore at different $[I_2/KI]$

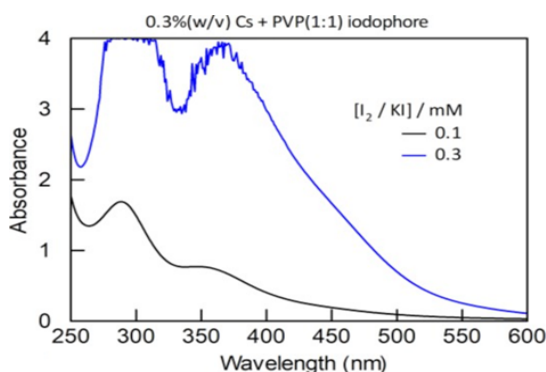


Fig. 14. UV-Visible Spectra of 0.3% (w/v) Cs+PVP (1:1)-iodophore at different $[I_2/KI]$

The complexation between the Cs+PVP (1:1) mixture with iodine is easily explainable at 0.1mM of I_2/KI solution and 0.1% of the Cs+PVP (1:1) mixture, as is evident from the spectra in Figs. 12-14. The formation of the iodophor persists between 0.3mM of iodine (I_2/KI) and 0.5% of Cs+PVP

(1:1) mixture at higher concentrations of iodine and polymer mixture, Fig. 15. This aberrant behaviour of the iodophor complex at 0.5% Cs+PVP (1:1) is similar to that observed in the spectra of the solution and complex of 0.5% Cs-iodophor at 0.1mM Iodine (I_2/KI). It may be worth mentioning that, to date, no reliable reports have been made available for comparison with the present study.

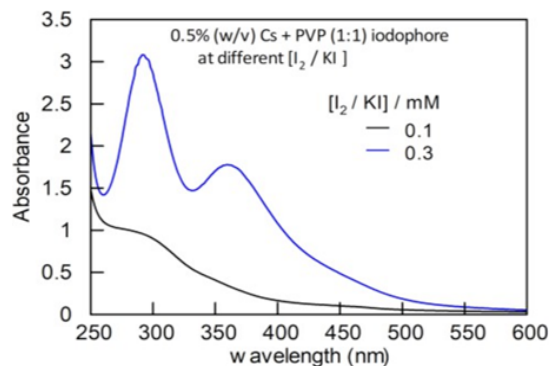


Fig. 15. UV-Visible Spectra of 0.5% (w/v) Cs+PVP (1:1)-iodophore at different I_2/KI concentration

Figure 16 shows the UV-Visible spectra of the Cs-iodophor solution in addition to 0.02% KSCN. The absorption maxima observed at 287.5 and 351nm of the Cs iodophor solution reduced with time and completed the reduction within 1 h of the observation. The concentration of the Cs, Iodine and KSCN used during the investigation has been chosen as the optimal concentrations from the experimental spectra shown in Figure 1-4.

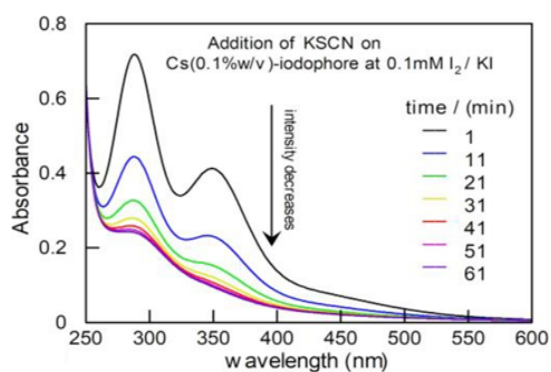


Fig. 16. UV-Visible Spectra of Cs-iodophore degradation on addition of 0.02% KSCN with time

It is pertinent to note here that the presentation of variation of absorbance with wavelength, even when the absorbance values shown beyond 3 in Figs. 6-9 and 14-16, serves as justification for the chosen concentrations of I_2/KI , Cs-iodophor, and polymer mixture-iodophor

for the present study. The concentration of the I_2/KI solution was chosen to be 0.1 mM. Various trial experiments confirmed that at this level, the iodophore concentration in the I_2/KI solution exhibits optimal absorption maxima when forming a complex with Cs or a Cs-polymer mixture at a 1:1 ratio, even up to certain higher concentrations. However, when the concentration of the I_2/KI solution is increased, good spectra are limited only to lower concentrations of the polymer or polymer mixture under investigation. Additionally, the addition of KSCN at 0.02% still shows clear spectra with reasonable absorption and stability for a certain period of time in the iodophore complex, beyond which it does not.

A full excitation scan conducted in the wavelength range of 280-900nm is to determine the excitation wavelengths for subsequent emission spectra measurements of Cs-iodophor in the acetic acid medium. It detected peaks at 700nm only for Cs-iodophor with higher I_2/KI concentration (0.3-0.5 mM) and two peaks at 349 and 700nm for Cs-iodophor with lower I_2/KI concentration (0.1mM). Interestingly, no emission peaks for Cs-iodophor were discernible when excited at 349 nm. Another peculiar behaviour is that no emission peak is observed at around 350nm, but at 701.4nm at increasing concentrations of I_2/KI in the Cs-iodophore (Fig. 25 included in supplementary material). However, emission peaks were identified at 350.5nm (3.54 eV) and 701.5nm (1.77 eV) when excited at 700nm (1.775 eV) as shown in the Fig. 21. The observed phenomenon lacks any references or pertinent literature for comparison. The observed peaks at 350.5nm (3.54 eV) are relatively smaller in intensity than the peak shown at 701.5nm (1.77 eV). The changes in the intensity of the emission peaks at 350.5nm (3.54 eV) and 701.5nm (1.77 eV) at different Cs concentrations while keeping the I_2/KI concentration fixed are shown in Fig. 22. It is observed from the Figure that the intensity of the emission peak increases with an increase in the concentration of the Cs.

DISCUSSION

The characteristic band reported at around 290 and 350nm is due to tri-iodide I_3^- ^{12,13} or

linear polyiodide I_5^- ion.¹⁴ Thus absorption peaks observed in the Cs-iodine solution contains I_3^- and linear I_5^- iodide ions and the peaks are prominent up to 0.5% w/v of Cs in the Cs-iodine system, Fig. 3-8. The complexation behaviour at different concentrations of Cs at around 310nm has shown a linearity, Fig. 5. The higher absorbance of the characteristic bands of the Cs-iodine complex indicates the presence of large interstitial spaces in the polymer aggregates, i.e., at higher concentrations wherein iodine enters and converts into polyiodides/polyiodine.^{15,16} From Fig. 4, the Cs-iodophor complex suggests interaction through I_3^- since no additional absorption maxima were observed. Formation of the Cs-iodophor complex further requires a large amount of iodine to release I_3^- and fill a large matrix of the polymer Figures 6-8.

Absorption maxima at ~301 and 387nm for Cs+PVP (1:1)-iodophor complex Fig. 10 would suggest that polymer mixture interacts with I_3^- and some other form of polyiodide ion during complexation. In contrast to the Cs-iodophor complex, the Cs+PVP-iodophor complex involves an additional polyiodide species, as evidenced by the observation of a new absorption maxima at 387nm. This absorption maximum at 387nm may be due to the participation of linear polyiodide ions during complexation.¹⁴ The increased absorbance at higher concentrations of iodine (I_2/KI) or polymer mixture (Figure 12-15) suggests that a specific proportion of the polymer mixture or I_2/KI solution is necessary to provide sufficient space for the integration of polyiodide ions into polymer mixture-iodophore. This suggestion is supported by the observation of absorption maximum at 292 and 368nm within the permissible range of the instrument when the iodophor is formed between 0.5% w/v Cs+PVP (1:1) and 0.3mM I_2/KI .

Kinetic study of the complex on addition of KSCN

The study of the plot of $x/A_0(A_0-x)$ vs. time⁹ at 287.5nm shows 2nd-order kinetics by considering the straight part of the plot until 31 min, after which it is observed to saturate Fig. 17. However, a kinetic study was not performed at 351nm because the reduction of the absorption maxima appears saturated beyond 10 min, and insufficient data on absorption maxima were observed, Fig. 16. Observations show that

both the thiocyanate and Cs-iodophor are relatively involved during the degradation of the Cs-iodophor. In the Cs+PVP (1:1)-iodophor system, the addition of KSCN reduces absorption maxima at 292 and 368nm Fig. 18. The degradation nature of the Cs+PVP (1:1)-iodophor by 0.02% KSCN is well defined till 61 minutes. The plot of $x/A_0 (A_0-x)$ vs. time of the polymer mixture-iodophor for the degradation process is shown in Fig. 19, indicating a linear trend at 292 and 368nm and extended throughout the reaction. This degradation pattern of the Cs+PVP (1:1)-iodophor by KSCN can be delayed until 61 min by maintaining the iodophor's complex form, as observed in Fig. 19 and 20. The distinct behaviour exhibited by the significantly higher absorption of the polymer mixture-iodophore upon the addition of KSCN facilitates the study of the system's kinetic behaviour. The degradation study at 292nm appears to follow a prominent 2nd order kinetic pattern compared to 368nm. To the best our knowledge, this behaviour of the polymer mixture-iodophor, has not been reported earlier.

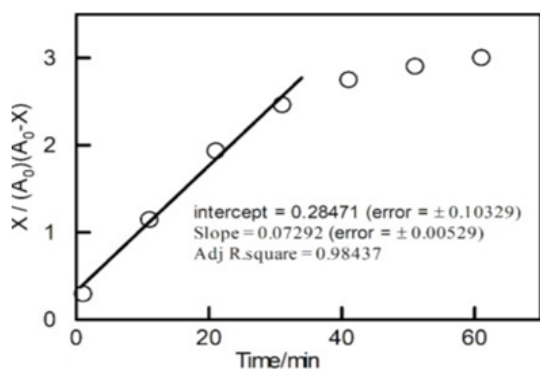


Fig. 17. Kinetic study of the Cs-iodophore on addition of 0.02% KSCN at 287.5nm

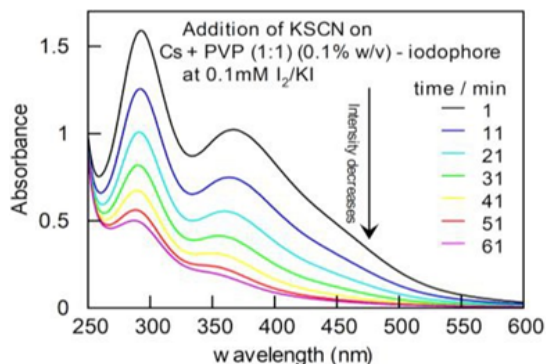


Fig. 18. UV-Visible Spectra of 0.1% (w/v) Cs+PVP (1:1)-iodophore degradation on addition KSCN (0.02%) with time

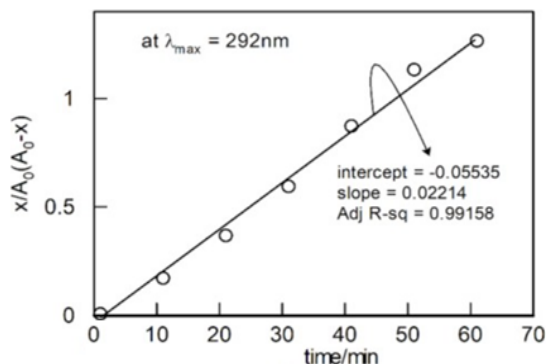


Fig. 19. Kinetic study of the 0.1% (w/v) Cs+PVP (1:1)-iodophore on addition of 0.02% KSCN at 292nm

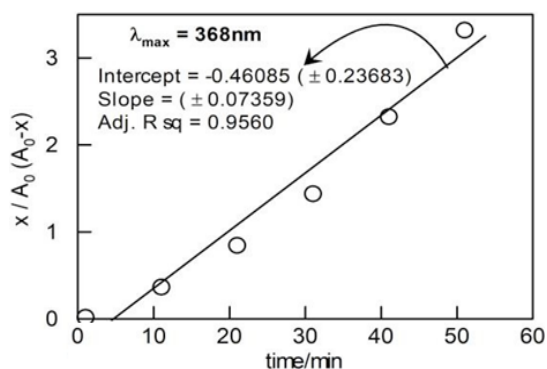


Fig. 20. Kinetic study of the 0.1% (w/v) Cs+PVP (1:1)-iodophore on addition of 0.02% KSCN at 368nm

Photoluminescence (PL) study of the Chitosan-iodophor

The observation of the higher intensity of the emission peak at 701.5nm (1.77 eV) in Fig. 21 has indicated a higher emission rate or presence of a higher concentration of emitting species. Both the emission peaks are sharp and narrow, indicating well-defined emissions. The I₂/KI solution forming iodophor with Cs at different concentrations has shown similar sharp and narrow emission peaks with higher intensity at the same wavelengths 350.5nm (3.54 eV) and 701.5nm (1.77eV) of the iodine solution, Fig. 22. The presence of two emission peaks at different wavelengths (350.5 and 701.5nm) indicates the possibility of two distinct fluorescent species within the solution, different energy transitions within the solution, or an indication of the complex electronic structure of the iodophor. The observations suggest that the I₂/KI solution and the Cs-iodophor exhibit fluorescence when excited at 700nm. The well-defined two emission peaks may be

associated with vibronic transitions 0 0 and 0 1 Fig. 23.¹⁷ The sharp and narrow emission peaks at 350.5nm (3.54 eV) and 701.5nm (1.77 eV) indicate a high degree of spectral purity.¹⁸ These observations suggested that the emission processes involve well-defined electronic transitions with minimal broadening. The narrowness of the emission peaks, coupled with specific wavelengths, implies that the I₂/KI is relatively pure and homogeneous and opens up potential applications in devices such as lasers, sensors, or optoelectronic systems. An increased Cs concentration may raise the probabilities of radiative transitions, consequently enhancing emission intensity at specific wavelengths. Additionally, as the concentration of Cs increases, the proximity of emitter's rises, fostering interactions such as energy transfer, intensifying emission at the same wavelength, and augmenting stimulated emission, ultimately enhancing the overall emission spectrum intensity at a given wavelength.

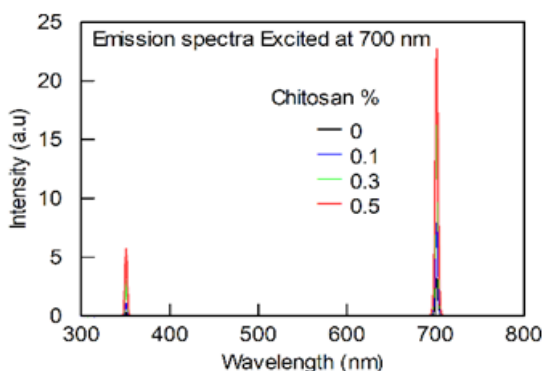


Fig. 21. Emission spectra of Cs-iodophore and I₂/KI solution excited at 700nm

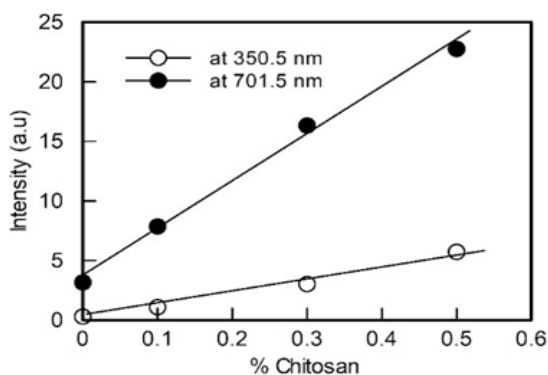


Fig. 22. Variation of intensity and Cs concentration for emission peaks of 350.5 and 701.5nm excited at 700nm

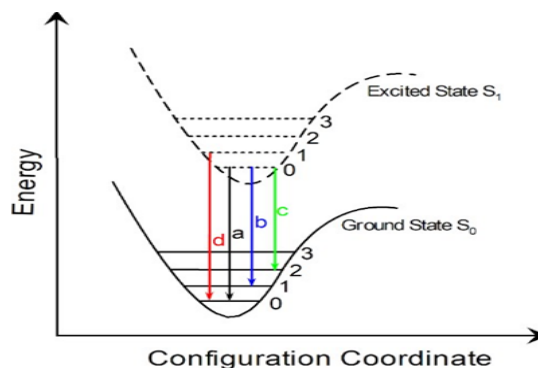


Fig. 23. Vibronic transition of the emission peaks of 350.5 and 701.5nm excited at 700nm

The correlation between the observed absorption maxima at 287.5 and 351.5nm Fig. 3 and emission peaks at 350.5 and 701.5nm, Fig. 21 indicates that the emission processes are related to specific electronic transitions responsible for absorption.¹⁹ The sharp emission peaks indicate efficient radiative recombination of excited electrons and holes. In addition, the smaller Stokes shift, which reflects minimal energy loss during the relaxation process, further emphasizes the efficiency of radiative recombination.²⁰ Stokes's shift is the separation between the wavelength of the absorption peak and the wavelength of the peak emission of a substance. The close match between excitation wavelength and emission peaks suggests potential fluorescence involving the absorption of photons followed by emission at longer wavelengths.

CONCLUSION

The Cs-iodophor exhibits absorption maxima at 287.5 and 351.5nm, attributed to tri-iodide I₃⁻ and linear I₅⁻ ions, as observed in the UV-Visible spectra. A new absorption maximum at 310nm indicates the formation of the Cs-iodophor complex thereby suggesting stability and potential use in wound management. The slow sustained release iodine from iodophor can help prevent and treat microbial infections in superficial and shallow-depth wounds. With increasing Cs concentration, there is a linear augmentation in iodophor formation, providing larger interstitial spaces for iodine integration. Additionally, iodophor with Cs+PVP (1:1) manifests absorption maxima at 292 and 368nm, which diminishes beyond 0.3% (w/v) polymer mixture. Thus Cs+PVP (1:1)-iodophor may have specific applications, especially considering

the polymer mixture effect. The degradation kinetics of Cs-iodophor and Cs+PVP (1:1)-iodophor by KSCN adhere to second-order kinetics, signifying their participation in degradation reactions. This information could be relevant for designing controlled-release systems or drug delivery applications. PL studies have revealed emission peaks at 350.5 and 701.5nm, showcasing distinct fluorescent species or energy transitions within the iodophor. The intensity of emission peaks increases with higher Cs concentrations, suggesting enhanced radiative transitions and potential applications in optoelectronic systems. The correlation between absorption maxima and emission peaks underscores specific electronic transitions responsible for absorption and fluorescence. Appearance of sharp emission peaks

indicates efficient radiative recombination, minimizing energy loss and hinting at potential fluorescence applications across various fields.

ACKNOWLEDGMENT

The authors extend heartfelt appreciation to Dr. Sanasam Bidaswar Singh of Thoubal College, Manipur for generously facilitating access to the Hitachi F-4700 Fluorescence Spectrophotometer for the present study. His support was instrumental in advancing our research and significantly enriching its quality and depth.

Conflict of Interest

We have no competing interests.

REFERENCES

- Chen, S.; Jiang, Y.; Wang, W.; Chen, J.; Zhu, J. The Effect and Mechanism of Iodophors on the Adhesion and Virulence of *Staphylococcus Aureus* Biofilms Attached to Artificial Joint Materials., *J. Orthop. Surg. Res.*, **2023**, *18*(1), 1–10. <https://doi.org/10.1186/s13018-023-04246-x>.
- Lim, S. H.; Hudson, S. M. Review of Chitosan and Its Derivatives as Antimicrobial Agents and Their Uses as Textile Chemicals., *J. Macromol. Sci.-Polym. Rev.*, **2003**, *43*(2), 223–269. <https://doi.org/10.1081/MC-120020161>.
- Yajima, H.; Morita, M.; Hashimoto, M.; Sashiwa, H.; Kikuchi, T.; Ishii, T. Complex Formation of Chitosan with Iodine and Its Structure and Spectroscopic Properties-Molecular Assembly and Thermal Hysteresis Behavior., *Int. J. Thermophys.*, **2001**, *22*(4), 1265–1283. <https://doi.org/10.1023/A:1010628712529>.
- Ke, C. L.; Deng, F. S.; Chuang, C. Y.; Lin, C. H. Antimicrobial Actions and Applications of Chitosan., *Polymers (Basel)*, **2021**, *13*(6). <https://doi.org/10.3390/polym13060904>.
- Ardean, C.; Davidescu, C. M.; Neme, N. S.; Negrea, A.; Ciopec, M.; Duteanu, N.; Negrea, P.; Duda seiman, D.; Musta, V. Factors Influencing the Antibacterial Activity of Chitosan and Chitosan Modified by Functionalization., *Int. J. Mol. Sci.*, **2021**, *22*(14). <https://doi.org/10.3390/ijms22147449>.
- Makhayeva, D. N.; Irmukhametova, G. S.; Khutoryanskiy, V. V. Polymeric Iodophors: Preparation, Properties, and Biomedical Applications., *Rev. J. Chem.*, **2020**, *10* (1–2), 40–57. <https://doi.org/10.1134/s2079978020010033>.
- Shipovskaya, A. B.; Fomina, V. I.; Solonina, N. A.; Yusupova, K. A. Preparation of Water-Soluble Chitosan Derivatives by Modification of the Polymer in Vapors of Monobasic Acids., *Russ. J. Appl. Chem.*, **2012**, *85*(1), 120–127. <https://doi.org/10.1134/S1070427212010235>.
- Shipovskaya, A. B.; Gegel', N. O.; Shchegolev, S. Y. Modification of Cellulose Acetates for Preparing Chiral Sorbents., *Russ. J. Appl. Chem.*, **2014**, *87*(9), 1326–1333. <https://doi.org/10.1134/S1070427214090225>.
- Cornell, H. J.; Rix, C. J. The Influence of Thiocyanate Ions on the Formation of the Starch-Iodine Complex., *Starch/Staerke*, **2006**, *58*(2), 100–108. <https://doi.org/10.1002/star.200500414>.
- Liyi Huang.; Weijun Xuan.; Tadeusz Sarna.; M. R. H. Comparison of Thiocyanate and Selenoc., *J Biophotonics*, **2019**, *12*(1), 1–22. <https://doi.org/10.1002/jbio.201800092>. Comparison.
- Chandler, J. D.; Day, B. J. Thiocyanate: A Potentially Useful Therapeutic Agent with Host Defense and Antioxidant Properties., *Biochem. Pharmacol.*, **2012**, *84*(11), 1381–1387. <https://doi.org/10.1016/j.bcp.2012.07.029>.

12. Noguchi, H.; Jodai, H.; Ito, Y.; Tamura, S.; Matsuzawa, S. Influence of Syndiotacticity on Poly(Vinyl Alcohol)-Iodine Complex Formation., *Polym. Int.*, **1997**, *42*(3), 315–320. [https://doi.org/10.1002/\(SICI\)1097-0126\(199703\)42:3<315::AID-PI735>3.0.CO;2-3](https://doi.org/10.1002/(SICI)1097-0126(199703)42:3<315::AID-PI735>3.0.CO;2-3).
13. Naorem, H.; Singh, N. S. Effect of an Anionic Surfactant on the Complexation of Some Nonionic Polymers with Iodine in Aqueous Media., *J. Phys. Chem. B.*, **2007**, *111*(16), 4098–4102. <https://doi.org/10.1021/jp067471d>.
14. Xu, X.; Guan, Y. Investigating the Complexation and Release Behaviors of Iodine in Poly(Vinylpyrrolidone)-Iodine Systems through Experimental and Computational Approaches., *Ind. Eng. Chem. Res.*, **2020**, *59*(52), 22667–22676. <https://doi.org/10.1021/acs.iecr.0c04766>.
15. Shipovskaya, A. B.; Malinkina, O. N.; Fomina, V. I.; Rudenko, D. A.; Shchegolev, S. Y. Optical Activity of Solutions and Films of Chitosan Acetate., *Russ. Chem. Bull.*, **2015**, *64*(5), 1172–1177. <https://doi.org/10.1007/s11172-015-0995-2>.
16. Chen, S. A.; Chan, W. C. Mechanism of Iodine Vapor Sorption in Polyacetylene., *J. Polym. Res.*, **1994**, *1*(4), 385–392. <https://doi.org/10.1007/BF01378772>.
17. Bakueva, L.; Matheson, D.; Musikhin, S.; Sargent, E. H. Luminescence of Pure and Iodine Doped PPV: Internal Energetic Structure Revealed through Spectral Signatures., *Synth. Met.*, **2002**, *126*(2–3), 207–211. [https://doi.org/10.1016/S0379-6779\(01\)00561-6](https://doi.org/10.1016/S0379-6779(01)00561-6).
18. Brunner, K.; Abstreiter, G.; Böhm, G.; Tränkle, G.; Weimann, G. Sharp-Line Photoluminescence of Excitons Localized at GaAs/AlGaAs Quantum Well Inhomogeneities., *Appl. Phys. Lett.*, **1994**, *64*(24), 3320–3322. <https://doi.org/10.1063/1.111265>.
19. Mamede, R.; Pereira, F.; Sousa, J. A. De. Machine Learning Prediction of UV–Vis Spectra Features of Organic Compounds Related to Photoreactive Potential., *Sci. Rep.*, **2021**, 1–11. <https://doi.org/10.1038/s41598-021-03070-9>.
20. Goetz, K. P.; Taylor, A. D.; Paulus, F.; Vaynzof, Y. Shining Light on the Photoluminescence Properties of Metal Halide Perovskites., *Adv. Funct. Mater.*, **2020**, *30*(23). <https://doi.org/10.1002/adfm.201910004>.